# Digital Image Processing Techniques for Object Tracking System Using Kalman Filter

**Kiran .S. Khandare[1], Nilima R. Kharsan[2]**

[1, 2]Department of Electronics & Telecommunication Engineering DES's COET Dhamangaon Rly

**Abstract:** *The focus of this paper is to design an algorithm to track an object, moving with an unknown trajectory, within the camera's field of view. To achieve this Kalman Filter (KF) is used for tracking and estimation because of its simplicity, optimality, tractability and robustness .It is also known as linear quadratic estimation (LQE). The Kalman filter, defined by simulation was applied to a DVT sensor to determine the actual performance. The Single Filter method was implemented. The Single Filter was able to track high speed an error of a couple pixels. By using this algorithm a series of measurements observed over time, containing noise (random variations) and other inaccuracies, and produces estimates of unknown variables that tend to be more precise than those based on a single measurement alone. It will helpful to track an object, moving with an unknown trajectory, within the camera's field of view (FOV). The Kalman filter uses the measured position of the target's centroid as well as previous state estimates to determine the position of the centroid in the next time step. More formally, the Kalman filter operates recursively on streams of noisy input data to produce a statistically optimal estimate of the underlying system state.*

**Keywords:** Field of View (FOV), Linear Quadratic Equation (LQE), Kalman Filter (KF).

## 1. Introduction

A design of Kalman Filter and its performance is tested in a simulation process. By using Newton's Second Law, A third order discrete model of the target is developed .A sine wave is used as the test trajectory to test filter's performance for simulation, using actual trajectory data. The filter was later refined, for experimentation. To enhance the performance, a new scheme, having two sets of filters, was developed. One filter work on the smart sensor and will predict the position of the target at the cameras sampling frequency. The second filter would work on the controller. It measure values at the same rate as the DVT sensor, but a target position predicted a higher sampling frequency. The scheme was not used however, the result of simulation indicate that this scheme gives greater precision at a higher sampling frequency.

## 2. Object Modeling For Kalman Filter

For creating Kalman filter an appropriate linear model of the target must be created. The model describes the x and y coordinates of the target centroid and also the orientation of the target. Every parameter is independent of each other. The x model and y model are same and it is based on Newton's second law. The Orientation is based on a moment equation. Now Consider Newton's second law, since each position coordinate is linearly independent then it can be partitioned:

$$Fx = max \qquad (1)$$
$$Fy = may \qquad (2)$$
$$Fz = maz \qquad (3)$$

The image only moves in two dimensions so the z component can be ignored. In an image the masses of an object, is the sum of all its pixels. As this model describes the centroid then its mass is unity. Therefore, the system reduces to:

$$Fx = ax \qquad (4)$$
$$Fy = ay \qquad (5)$$

It is sufficient to examine only one of these components and apply an identical model to each. Let us consider the generalized system, F = a. In this, the system appears to be second order with respect to position. However, If it is stated that the force and acceleration vary with time then the system is defined as F(t) = a(t). Take the derivative of this equation and the result is a third order equation that describes the jerk of the object.

$$\begin{bmatrix} \dot{x} \\ \dot{v} \\ \dot{a} \end{bmatrix} = \begin{bmatrix} 0 & 1 & 0 \\ 0 & 0 & 1 \\ 0 & 0 & 0 \end{bmatrix} \begin{bmatrix} x \\ v \\ a \end{bmatrix} + \begin{bmatrix} 0 \\ 0 \\ 1 \end{bmatrix} \dot{F}$$

$$\begin{bmatrix} x_{k+1} \\ v_{k+1} \\ a_{k+1} \end{bmatrix} = \begin{bmatrix} 1 & T & T^2 \\ 0 & 1 & T \\ 0 & 0 & 1 \end{bmatrix} \begin{bmatrix} x_k \\ v_k \\ a_k \end{bmatrix} + \begin{bmatrix} \frac{T^3}{6} \\ \frac{T^2}{2} \\ T \end{bmatrix} J_k$$

Where T is nothing but the sampling period of the discretized system. Here no known input is applied to the target. Instead the object moves solely due to disturbances. Figures 1 and 2 show the predictor's performance at the chosen ratio. Figure 3 illustrates the tracking ability of the filter. This figure shows near perfect tracking. There is a slight phase lag and very little overshoot. Figure 4 shows the error between the trackers

and the real signal. The oscillations are due to the phase lag. But observe that the error is on the magnitude of fractions of a pixel.
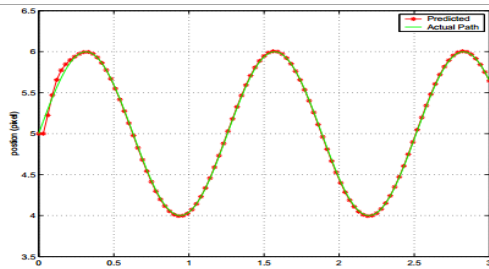
**Figure 1:**.Kalman Filter's Simulated Tracking Performance
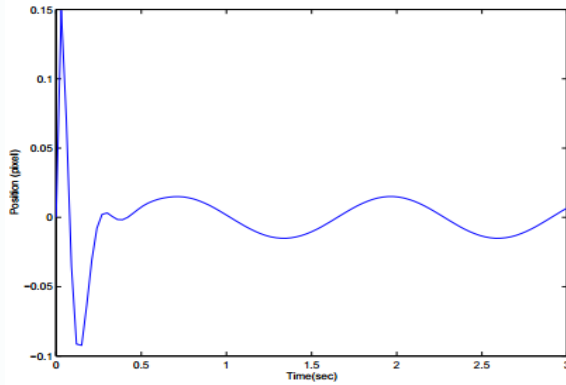


**Figure 2:**.Error Plot of the Filter Tracking the Sine Wave

For the sake of this example, the other processor will be located external to the DVT sensor and it is associated with a controller.

The Dual Filter is having two sets of filters. One set provides estimates for the smart sensor and the other set provides estimates for the controller. Figure4 shows a schematic of the setup. The Single Filter remains on the DVT. Another filter is run on a controller at a higher frequency. The DVT sensor, once every sample period, sends the measured values, which describe the target position, to the controller. The filter on the controller will hold this value until it is updated by the smart sensor. The process of holding the measurement value has the effect of creating another input trajectory that operates on the controller's frequency. Figure 5 illustrates an example of a new trajectory. In this example, the controller operates at frequency that is ten times faster than the camera filter. The controller filter will use the new input measurement function to determine the incremental estimates of the object. These estimates will be computed at a higher frequency. The higher frequency will be a multiple of the camera frequency. This is done to synchronize the transfer of measurement values**.** Data from actual target trajectories were used as test inputs.
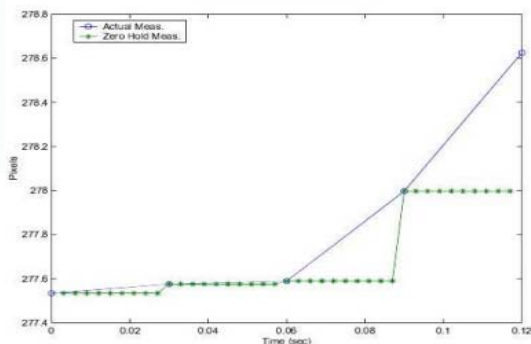


**Figure 3:**.Illustration of Dual Filter Measurements

This data included the coordinate positions of the target centroid and the orientation of the target. Beginning with a third order continuous time state-space model, two discrete state-space models were created. One was built with a sample time of 33Hz, and the other was designed for 3.3kHz. Kalman filters were computed for each of these two models and then both systems were closed.

The first Kalman filter, which will now be called the camera filter, is placed on the sensor. The second filter, labeled as the controller filter, is the predictor that will provide estimates in between each camera period. Note that the $3^1$s period is just an example.
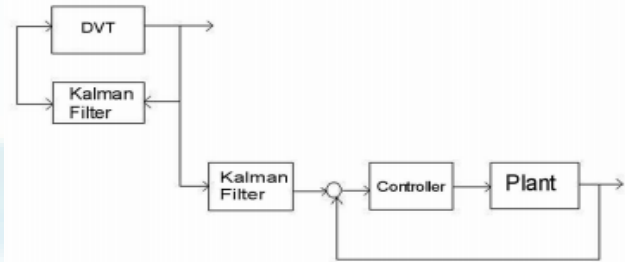


**Figure 4:** Block Diagram of Dual Filter System

An actual period would be determined by the processor speed of the controller and the transportation speed of data between the controller and DVT sensor. The simulated results of this setup are promising. The controller filter operates at a high frequency and with greater accuracy than the Single Filter. Since the input is not updated every time increment of the controller, it was assumed that the ratio of measurement noise to disturbance noise was smaller. Figure 9 compares the x-coordinate predictors of the camera and controller filters with the measured x-coordinate value they are tracking. This comparison is done at the camera sampling period. This plot gives an assessment of how well each predictor follows the measured value and allows for the comparison between the two filters. The camera filter exhibits a lag as well as overshoot when tracking the target. The controller filter, tracks the target with slightly smaller lag and a much smaller overshoot.
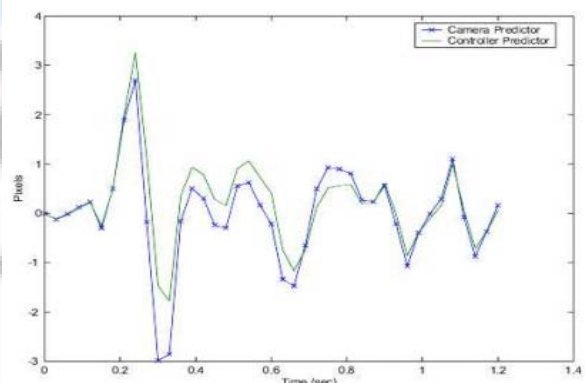


**Figure 5:** Error Comparison of Predictors in the X-coordinate

The comparison of the predictors in the X-coordinate is still needed in order to predict the partial window location of the next time step. The camera can communicate with external devices, but the timing of these communications is

secondary to the routines run on the DVT. So there is no guarantee that the signal from the controller will be received in time to adjust the field of view. So the camera filter is needed to place the sensor in the right region, while the controller sensor can be used to track the object. The controller filter is providing estimates in between sensor measurements.

Kalman gains, a disturbance to noise ratio was determined for the continuous model to compute the continuous Kalman gains. The system was then discretized. Consider the controller predictor of the proposed Dual Filter algorithm. Suppose this predictor operates at n times the sampling frequency of the DVT sensor. Let us restate the controller predictor:

$$x_{k+1} = [G \text{ ¡ } KC] x_k + Ku_k \tag{6}$$
$$x_{k+1} = G^- x_k + H^- u_k \tag{7}$$

where $G^- = G \text{ ¡ } KC$ and $H^- = K$. From now on the bars will be ignored so that G corresponds to $G^-$. Let us compute $x_{k+2}$:

$$x_{k+2} = Gx_{k+1} + Hu_{k+1} \tag{8}$$
$$= G [Gx_k + Hu_k] + Hu_{k+1} \tag{9}$$
$$= G2x_k + GHu_k + Hu_{k+1} \tag{10}$$

Recall that for the controller predictor, the measurement is constant until the camera's next time step. So $u_k = u_{k+1} = u_{k+2} = : : : = u_{k+n¡1}$ Therefore $x_{k+2} = G2x_k + [G + I] Hu_k \tag{11}$

Now consider $x_{k+3}$

$$x_{k+3} = Gx_{k+2} + Hu_{k+2} \tag{12}$$
$$= G2x_k + [G [G + I]] Hu_k + Hu_k \tag{13}$$
$$= G3x_k + £G2 + G + I¤Hu_k \tag{14}$$

And so a pattern emerges where:

$$x_{k+n} = Gnx_k + "nX_{¡1i=0}Gi\#Hu_k \tag{15}$$
$$x_{k+n} = G^\sim x_k + H^\sim u_k \tag{16}$$

where $G^\sim = Gn$ and $H^\sim = hPn_{¡1i=0} GiiH$.

Consider the linear continuous model of the target:

$$x^\cdot(t) = Ax(t) + Bw(t) \tag{17}$$
$$y(t) = Cx(t) + v(t) \tag{18}$$

Using equation 11, predictor type Kalman filter can be determined. This filter can then be discretized. In this case the zero-order hold method was used to discretize the continuous filter to a discrete filter with the sampling time of the DVT sensor Figure 6 shows the performance of a predictor that is built in continuous time.
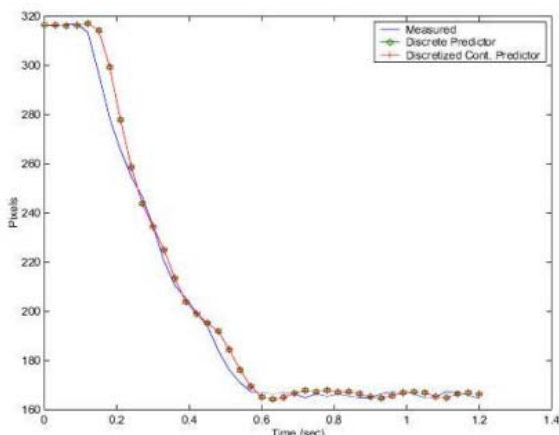


**Figure 6:**.Comparison of the Discretized Kalman Filter to a Discrete Kalman Filter
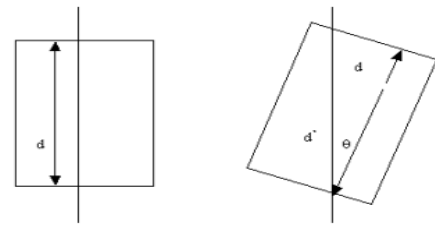
## 3. Methodology



**Figure 7:**.Method for Determining the Target Alignment

If the measured length is lower than the defined value the angle is set to zero. If this happens it is attributed to noise in the measurement. The sensor then loads the previous state predictions, which are now the current state estimates. The estimates and the measurements are applied to the state equations to determine the new prediction. The future estimates are loaded into the specified registers and overwrite the old estimates.
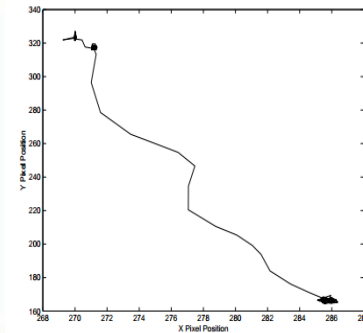


**Figure 8:**.An Example Trajectory of a Target

Figure 8.shows the ability of the filter to predict the x coordinate of the target's centroid. There is an overshoot when tracking fast changes in the x direction. An illustration of the performance can be seen in an error comparison. The objective is to track the measured signal, so it is assumed that the measure is the true coordinate position. So the error is the difference between the prediction and measured value. The error values are very low and within a band of §2 pixels. Part of the reason for this very low number is that the x coordinate was experienced medium velocities. The y coordinate, on the contrary, was exposed to higher speed
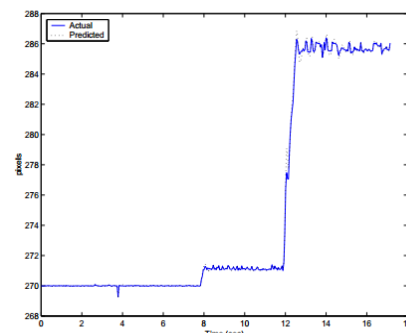


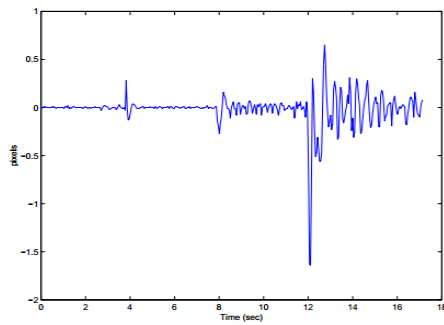**Figure 9:**.X-Coordinate Tracking of the Single Filter

**Figure 10:**.shows the X-Coordinate Tracking Error of the Single Filter.

y coordinate position as a function of time, and it shows the predictor's ability to track this trajectory. Figure 11 illustrates the y coordinate tracing performance. The error is relatively small. There is one overshoot of 12 pixels for the large motion, but all other measurements lie within §2 pixels.
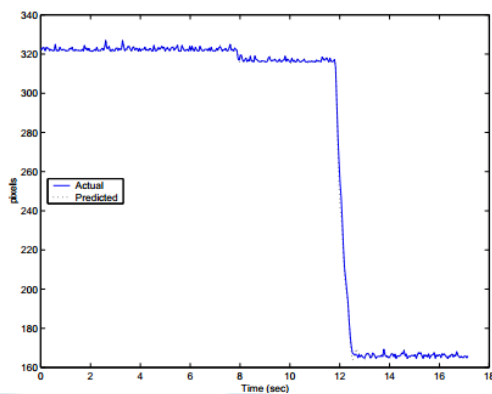


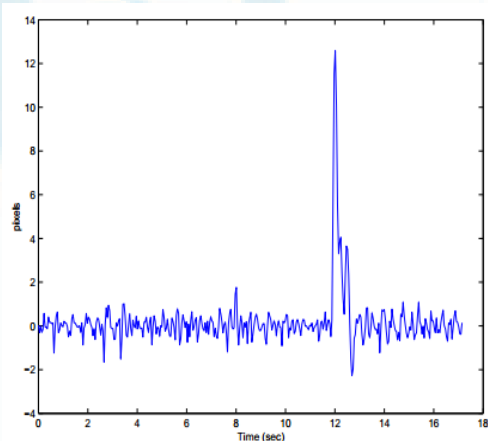**Figure 11:**.Y-Coordinate Tracking of the Single Filter



**Figure 12:**.Y-Coordinate Tracking Error of the Single Filter

The angle tracking was also good.Figure13 shows the predictors capability to predict the orientation. This trajectory does not undergo large angle changes. This was done since the angle measurement method was not designed for large angle changes**.** Observe the large oscillations in the angle. Some of the oscillations are due to actual orientation changes but another factor is the noise in the angle measurement itself. To compute the angle the process described in Image Processing Section is used. This was done for both the vertical and horizontal measurements. The

two angles computed were then averaged. However the noise in the vertical direction was too high. So for all subsequent implementations only the horizontal distance measurement was used to compute the measured angle.. The error was between §2o .



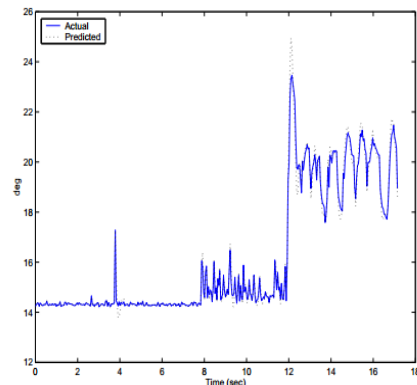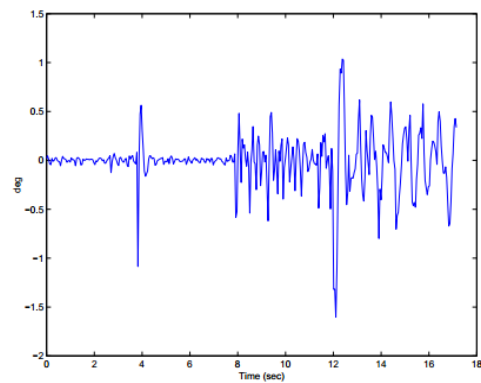**Figure 13:**.Angle Tracking of the Single Filter



**Figure 14:**.Angle Tracking Error of the Single Filter

## 4. Conclusion

Neither processing method was able to increase the sampling frequency to be sufficient for control applications. Since the actual frequency of vision measurements could not be improved further, another algorithm was created to provide accurate estimates in between vision measurements. The Dual Filter was designed to have a higher frequency Kalman filter run on the controller's processor. This design was simulated and yielded high accuracy estimates. In this case, the estimate frequency is limited only by the speed of the controller's processor itself. The Single Filter which provides one estimation per time period provided accurate predictions, usually between §10 pixels for large velocities.

## 5. Analysis of Performance Result

For each tracking method and each performance measure, 48 values could in principle be computed, corresponding to the 48 data cases (different combinations of particle dynamics, densities and signal levels). However, not all teams submitted tracking results for all cases, which ruled out the possibility to perform an overall comparison and ranking of the different methods based on all cases. We observed that teams who did not apply their method to all 48 cases generally focused on one or more of the four dynamics scenarios representing different biological applications, but

even per scenario not all teams applied their method to all pertaining cases. Therefore, we decided to rank the methods according to best performance per measure and per data case.

## 6. Verification of Tracking Results

Minor differences between the originally submitted tracking results and the verified results were to be expected because some of the software tools were converted to another platform to allow execution on the single evaluation system, and some methods were probabilistic in nature. Therefore, for each method, differences were considered acceptable (reproducible) if their means for each of $\alpha$, $\beta$, JSC and JSC$\theta$ were within 3% and the RMSE was within 0.5 pixel. In the vast majority of cases, the differences were acceptable, and the larger differences in some cases could be traced back to bug fixes and minor improvements in the software or parameter settings used for verification as compared to the original versions. In very few instances the results could not be verified owing to hardware or software limitations (Supplementary Table 3). For the analysis, the performance values computed from the originally submitted tracking results, not the verified results, were used.

## Reference

[1] Greg Welch and Gary Bishop. An introduction to the kalman filter. University of North Carolina at Chapel Hill, Department of Computer Science, Chapel Hill, NC,USA

[2] Saxton, M.J. & Jacobson, K. Single-particle tracking: applications to membrane dynamics.Annu. Rev. Biophys. Biomol. Struct. 26, 373–399 (1997).

[3] Akhmanova, A. & Steinmetz, M.O. Tracking the ends: a dynamic protein network controls the fate of microtubule tips. Nat. Rev. Mol. Cell Biol. 9, 309–322 (2008).

[4] Berginski, M.E., Vitriol, E.A., Hahn, K.M. & Gomez, S.M. High-resolution quantification of focal adhesion spatiotemporal dynamics in living cells. PLoS ONE 6, e22025 (2011).

[5] Brandenburg, B. & Zhuang, X. Virus trafficking– learning from single-virus tracking. Nat. Rev. Microbiol. 5, 197–208 (2007).

[6] Arthur Earl Bryson and Yu-Chi Ho. Applied Optimal Control. Hemisphere and Wiley, 1975.

[7] Peter I. Corke. Dynamic issues in robot visual- servo systems. J. Alg., 111:427–430, 1987.

[8] Peter I. Corke and Malcolm C. Good. Dynamic effects in high performance visual servoing. Proc. 1992 IEEE Int. Conf. Robotics and Automation, pages 1838–1843, 1992.

[9] DVT Corporation. Dvt script reference manual. 200

[10] DVT Corporation. Dvt framework 2.0  Smart image sensors installation & user guide. 2000.